$\gamma - \gamma$ Angular correlation

Navrit Bal

College of Letters and Science
University of California at Berkeley
Berkeley, California, U.S.A.

Nuclear Engineering 102
navrit@berkeley.edu

March 12, 2015

Abstract

We have verified the isotropic distribution of gamma emissions from a Cobalt-60 source by measuring the angular distribution of coincident gamma detections. We showed that the distribution was as predicted by a generalised result from group theory [2] which required knowledge of the nuclear spin states of Co-60. The motivation for this experiment is to directly show the manifestation of a particular quantum effect on a truly macroscopic scale. The angular resolution of the system was determined by using the highly precise, Sodium-22 positron annihilation events and was found to be $\sigma_\theta = \mathbf{14.6^\circ}$

Note: British English spelling is adhered to within this document.

1 Theory

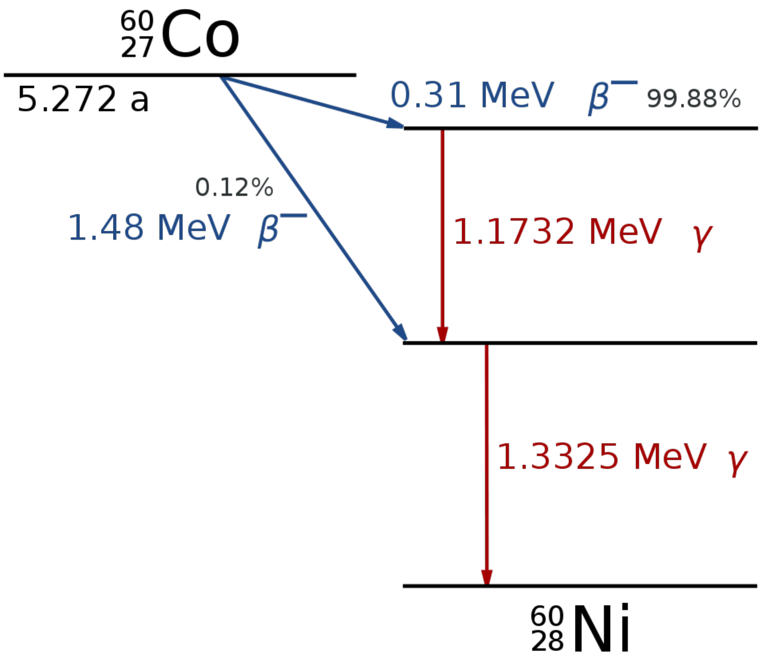

Figure 1: [1] Decay chain of Co-60 - showing gamma photon emission energies at 1.17 and 1.33 MeV with their respective decay probabilities and decay types. The lifetime of the 1.33 MeV state is 0.7ps. As shown, Co-60 has a half life ($t_{\frac{1}{2}} = 5.272\ years$).

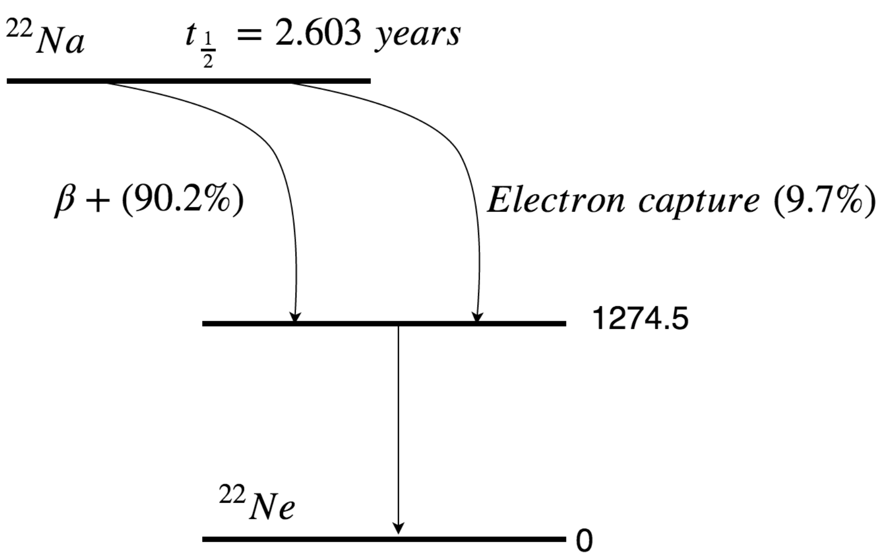

Figure 2: Decay chain of Na-22 - showing positron emission (Beta +) which will lead to gamma photon emission energies at 511 KeV due to annihilation events with electrons. As shown, Na-22 has a half life ($t_{\frac{1}{2}} = 2.603\ years$). There will also be a 1.2745 MeV gamma peak and probably x-rays from electron capture.

When a Co-60 nucleus decays via β - emission, it goes to one of 2 excited Ni-60 states as shown in Figure 1. 99.88% of the time the nucleus will decay by emitting a 0.31 MeV $\beta-$ particle (electron), then a 1.1732 MeV γ photon followed by a 1.3325 MeV photon at which point, it has become Ni-60. The lifetime of the intermediate 1.3325 MeV state is so short at 0.7ps, that due to the physics of the emission process, their directions are often correlated with each other. This is due to the spin of the nucleus being having an effect on the angular distribution of the emitted photons per transition. "The relative probability that a photon will be emitted at an angle θ with respect to a previously emitted photon is denoted W(θ) and depends both on the angular momenta of the states involved in the transitions and on the multipole order of the emitted radiation." [1] This is one way to achieve correlated γ photons.

When a Na-22 nucleus decays via $\beta+$ emission (90.2% 'f the time) as shown in Figure 2, that positron will soon annihilate with a nearby electron thus producing 2 correlated γ photons. Due to conservation of momentum, these γ photons are emitted at 180 from each other at this energy scale. A 1274.5 KeV emission will occur from the excited intermediate state of Ne-22.

Since the decay physics of Na-22 almost exclusively produce correlated γ photons, we use Na-22 for system calibration and determining the angular resolution of the system. The somewhat more complicated Co-60 situation can then be explored by measuring the angular distribution of counts along one axis.

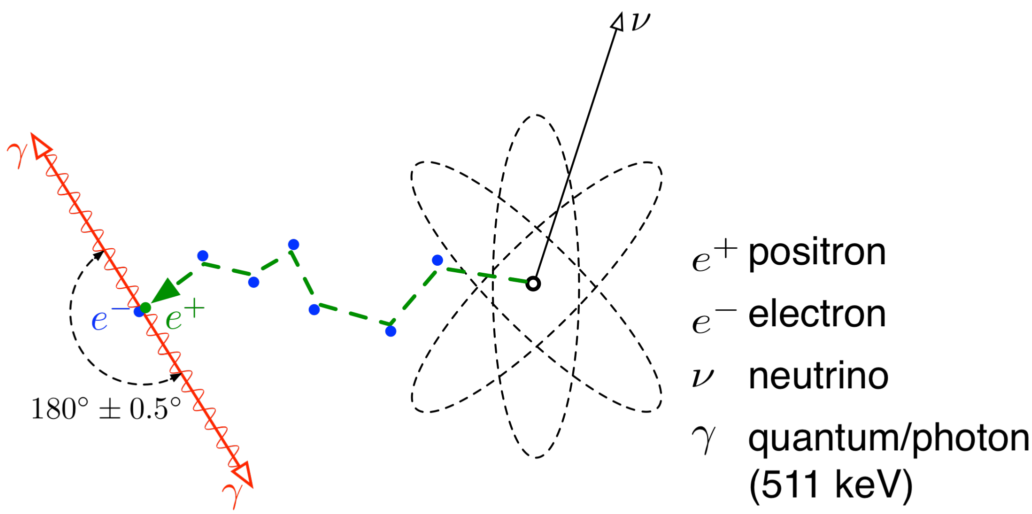

Figure 3: Diagram showing the annihilation process as a result of $\beta+$ emission from Na-22 with the subsequent 2 γ emissions at 180 from each other.

2 Experiment

2.1 Method and Procedure

1. Bias detectors to +700V
2. Load radioactive sample (Na-22 or Co-60)
3. Determine angular resolution of the system with Na-22

4. Measure angular correlation of Co-60

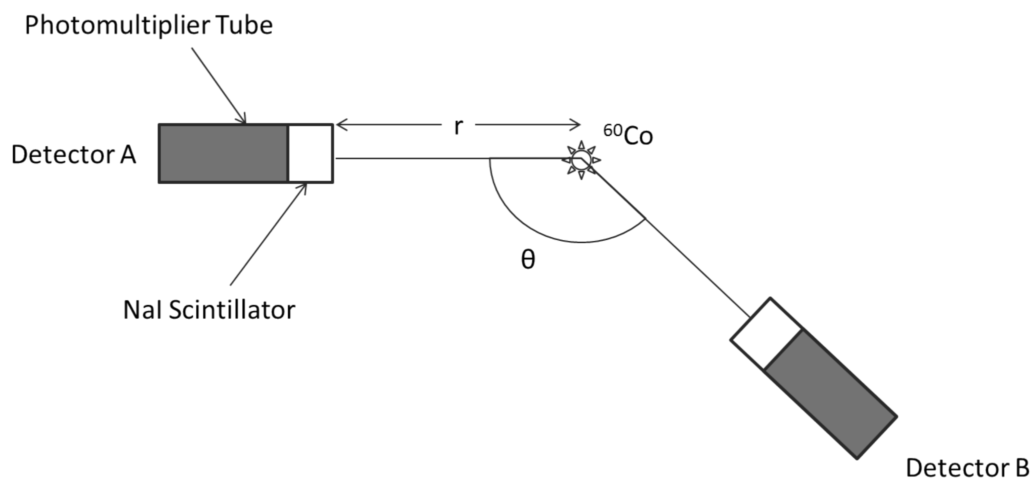

Figure 4: Diagram showing the physical layout the main our experiment - how the angle between the detectors is changed around the radioactive source. Our equipment used integrated detectors - the photomultipier tubes were within the same package as the scintillators.)

2.1.1 Electronics, experimental diagrams

1. Co-60 radioactive source - gamma photon emitter (1.17 and 1.33 MeV)
2. Na-22 radioactive source - positron emitters (511 KeV peak via annihilation events)
3. Pb bricks (gamma bricks)
4. 2 NaI Bicron 3M3/3 gamma detectors - scintillation detector with integrated mounted PMT (Photomultiplier Tube)
5. Multiple channel analyser (MCA) - (ORTEC Easy MCA)
6. Software - ORTEC Maestro MCA analyser
7. ORTEC NIM (Nuclear instrumentation modules) units
   (a) HV (High Voltage) PSU (Power supply unit)
   (b) Gate and delay generator
   (c) Dual spectroscopy amplifier (Dual Spec. Amp.)
   (d) 2 Single channel analysers (SCA)
   (e) Delay amplifier
   (f) Time to amplitude module (TAC)

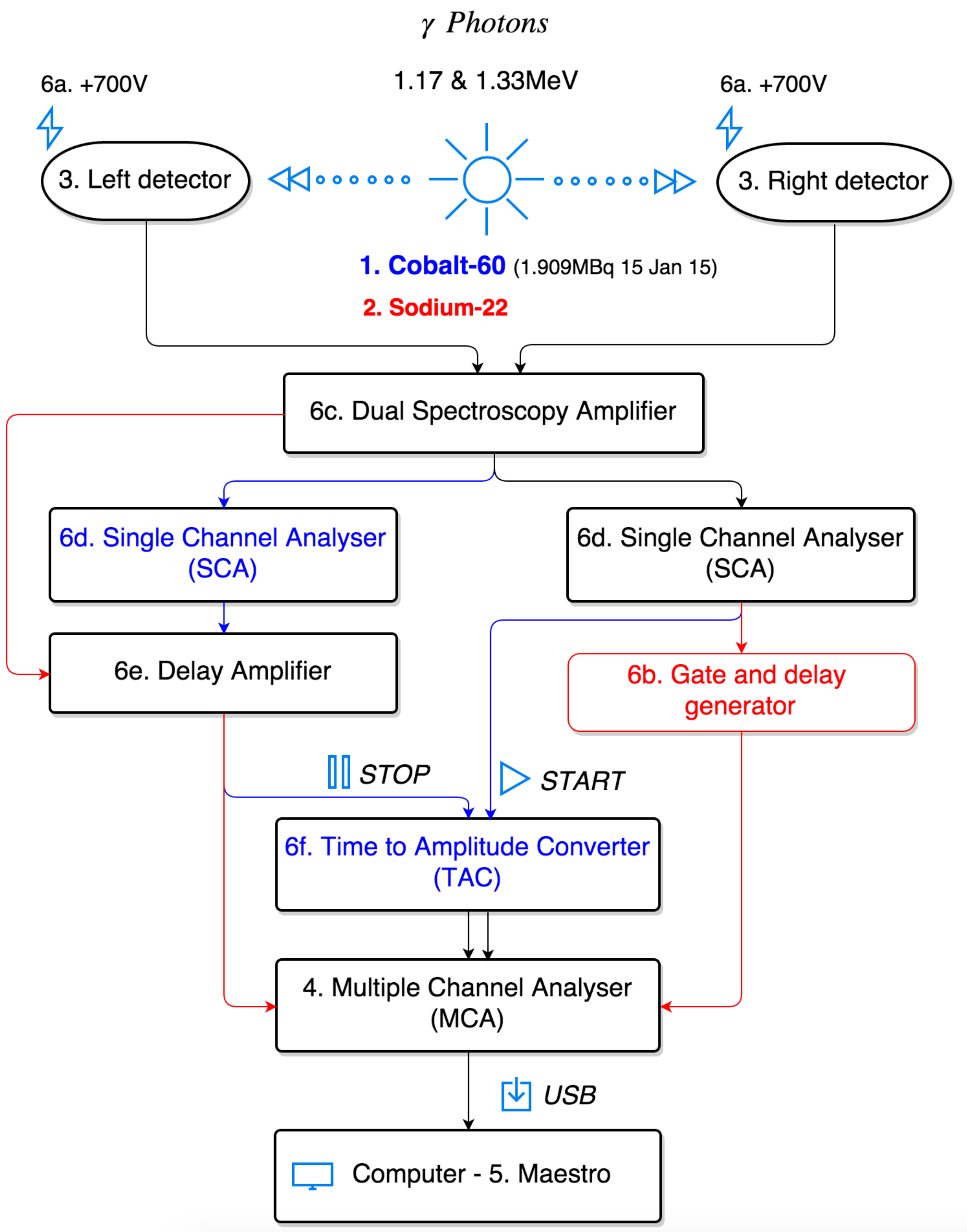

Figure 5: A logical overview diagram of the Co-60 (follow blue lines) and Na-22 (follow red lines) experimental setup. See 2.1.1 for a more comprehensive list.

2.2 Data

Na-22

θ Angle [º]	C(θ) Counts [unitless]	σ_C [s^{-1}]	t Acquisition Time [s]	σ_θ [º]
180.0	2567	50	200	1
179.0	2435	49	200	
177.5	2059	187	200	
175.0	1651	134	201	
172.5	1200	34	201	
170.0	687	26	200	
167.5	371	19	200	
165.0	71	8	215	
Measured	Measured	Maestro	Measured	Measured

Figure 6: Raw sodium-22 data.

Co-60

	Gross counts [unitless]				*Counts [unitless]*		*Relative count rate [unitless]*	
θ Angle [º]	P, Peak	L, Left bin	R, Right bin	B, Background	C(θ), Net Peak	σ_C	C(θ) / C(90º)	Theory [unitless]
180	3537	1110	1128	1119	2418	64	1.18	1.17
165	3443	1079	1089	1084	2359	63	1.15	1.15
150	3346	1049	1097	1073	2273	62	1.10	1.12
135	3284	1043	1030	1037	2248	62	1.09	1.07
120	3299	1076	1100	1088	2211	62	1.07	1.03
105	3061	1055	1069	1062	1999	60	0.97	1.01
90	3078	1028	1013	1021	2058	60	1.00	1.00
Measured	Measured	Measured	Measured	(L+R) / 2	P - B	√(P+B/2)	C(θ) / C(90º)	

Figure 7: Raw cobalt-60 data. The theory column is defined by $C(\theta) = 1+\frac{1}{8}cos^2(\theta)+\frac{1}{24}cos^4(\theta)$ [2]. B, C(θ) and σ_C are determined using the formulae from the distributed instructional slides for NE102 and the $\frac{C(\theta)}{C(90)}$ column is from Mellisinos.[2]

Constant values

Co-60	*Uncertainties*		
Acquisition time [s]	Acquisition Time [s]	θ Angle [º]	C(θº) / C(90º) [unitless]
900	2	14.6	0.03
Measured			

Figure 8: Uncertainty in acquisition time was based on measurements, the others were determined using various formulae which ar discussed in the Error analysis (2.4) section.

2.3 Analysis and Results

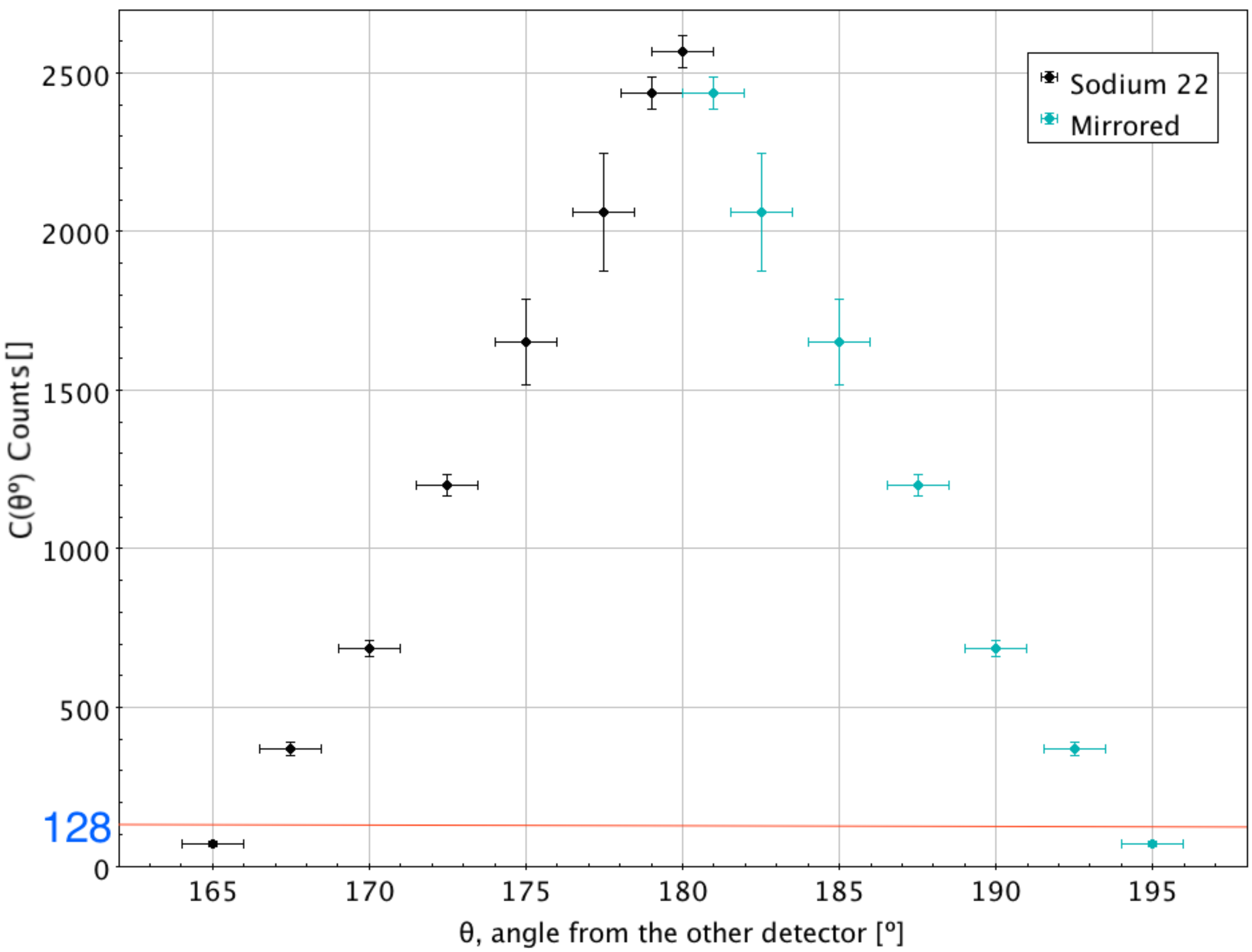

Figure 9: There is clearly a maximum in coincidence counts when the angle between the detectors is 180. This plot is used to determine the angular resolution of the system. The red line at counts 128 indicate the 5% mark of the maximum; this is discussed after. Counts is unitless since it is the number of events over 200s. The 'mirrored' points have been displayed purely for plotting purposes, only the points on the left half of the plot were measured - see figure 6 for the raw data.

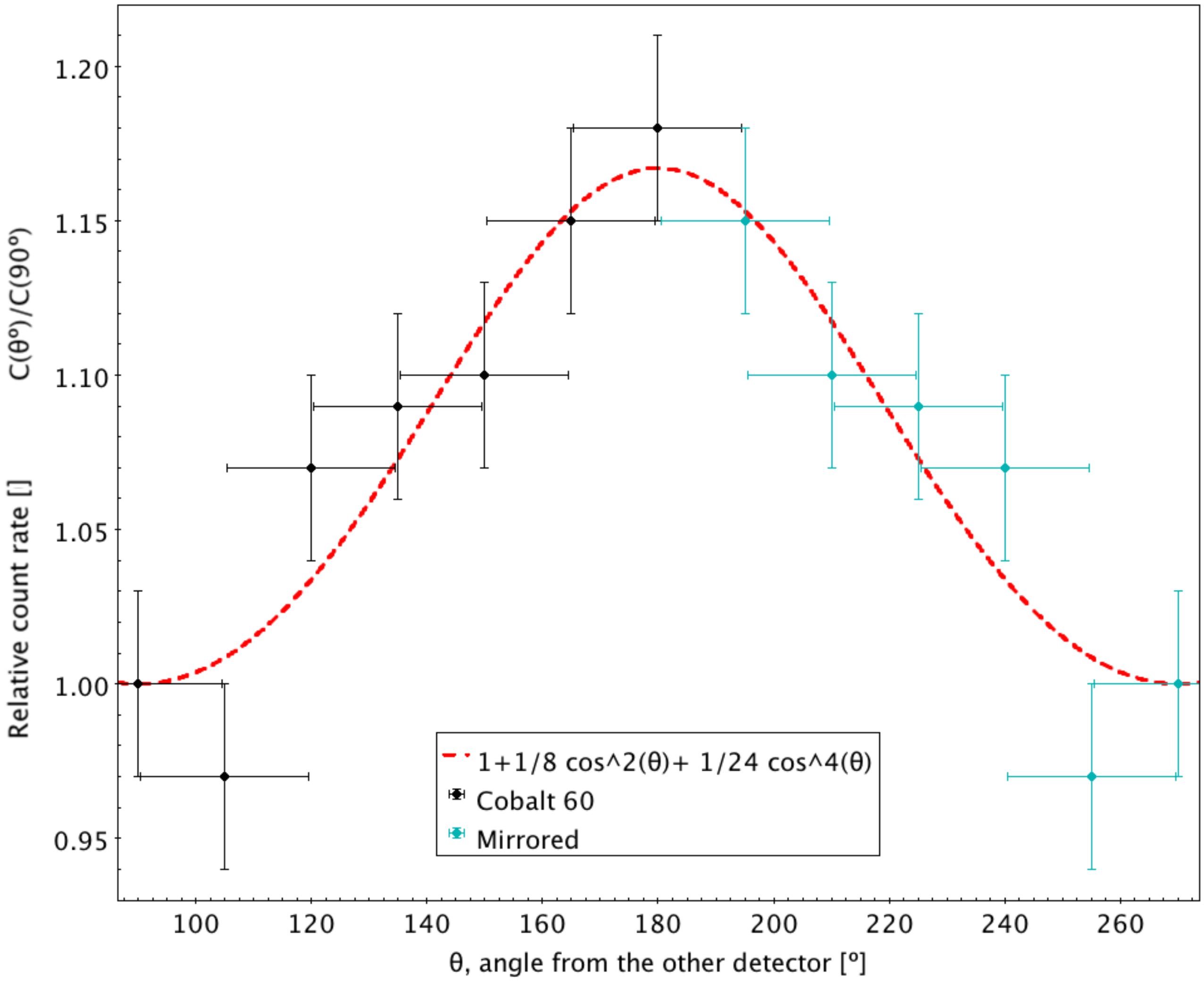

Figure 10: Relative counts is a unitless quantity because the coincidence counts (C) are both unitless numbers. The red dotted line is the theoretical curve as obtained from Mellisinos [2]. The 'mirrored' points have been displayed purely for plotting purposes, only the points on the left half of the plot were measured - see figure 7 for the raw data. The uncertainties are discussed in the Error Analysis section.

Figure 10 is verified by amongst many others, Mellisinos [2] (page 423 figure 9.25) and actually improves on that plot as we have plotted horizontal error bars which are the angular resolution of the system. The angular resolution for this plot (uncertainty in θ) was determined using the data from the Na-22 measurements to be $\boldsymbol{\sigma_\theta = 14.6°}$. Given all of the error bars, all of the data points fall within the expected boundaries as predicted by the $C(\theta) = 1 + 1/8\ cos^2(\theta) + 1/24\ cos^4(\theta)$ equation [2]. Whilst our data supports the theory, uncertainties prevent any further constraints on the theory.

An attempted Chi-square analysis of Cobalt-60 plot (figure 10) yielded a value of $\chi^2 = 24$ for $\nu = 7 - 1$ (degrees of freedom). The number of degrees of freedom was calculated with 7 data points minus 1 for the calculation of the variance. A right-tailed p-value for this result is then

$p = 0.0005$.The following equation was used for the analysis: $\chi^2 = \sum_{i=1}^{n} \frac{relative\ count\ rate_i - theory_i}{\sigma_i^2}$ - see figure 7

A minor point to note is the actual activity of the Co-60 sample was not the same at the time of using it as it was on 15 January 2015. The sample was mainly used 51 days after that date, and so a calculation of the estimated count rate on the day of primary usage is now presented with this information. The half life of Co-60 is 5.27 years ($t_{\frac{1}{2}} = H = 1925\ days$).

$$A = A_0\ 0.5^{\frac{t}{H}}$$

Where A = current activity, A_0 = activity at time t, t = time since reference activity (51 days) and H = the half life (1925 days)

$$A = 1.909\ MBq\ 0.5^{51\ d/1925\ d}$$

$$A = 1.874\ MBq$$

Given a detector efficiency ≈ 0.1, activity frequency ($A = 1.874\ MHz$) and solid angle per detector $(\frac{\pi R^2_{Detector}}{4\pi R^2_{Distance}})$, $R_{Detector} \approx 3in$, $R_{Distance} \approx 10in\ = \frac{9}{400}$ - the expected number of coicedent gamma detection events ($\gamma_{expected}$) can be calculated.

$$\gamma_{expected}\ (Frequency\ of\ seeing\ 2\ 1.3MeV\ \gamma\ photons) = (\frac{4}{900})^2 * 0.1^2 * 1.874\ MHz \approx 10Hz$$

2.4 Error Analysis

The Na-22 uncertainty in angle (figure 6) was just due to measurement limitations, the markers on the table were every 2.5° from 180° to 170°. The uncertainty in counts (σ_C) were taken straight from Maestro without any further modification. For most of the measurements, this uncertainty in counts ($C(\theta)$) appears to be the correct values . The correct calculation of the uncertainty in count should have been $\sigma_C = \sqrt{C}$ where C is the total count. Maestro appeared to have followed the correct method with the exception of the 177.5 and 175.0 measurements. The cause of this is unknown.

As shown in figure 7, the uncertainty in the number of counts (σ_C) has been calculated by the method shown in the distributed slides for this class ($\sigma_C = \sqrt{Peak + \frac{Background}{2}}$). The uncertainty in the ratios of the count rate at an angle to the count rate at 90 degrees was constant at $\frac{C(\theta)}{C(90)} = 0.03$ [$unitless$] (1 significant figure). This was calculated by $\frac{\sigma_C}{C(\theta)} \approx 0.03$ - see figure 7. The angular resolution (σ_θ) was calculated with the same method as found in Mellisinos [2] and is briefly outlined as follows:

$$\sigma_{\theta - Na22} = 180° - 165° - \frac{0.05 * Peak - C(165°)}{\frac{C(167.5°) - C(165°)}{167.5° - 165°}} = 15° - \frac{0.05 * 2567 - 71}{\frac{371-71}{167.5-165}} = 14.5° = 14.5°$$

This then has to be combined by quadrature with the angular uncertainty of the detector $\sigma_{\text{det.}} = 2°$ - this is from measurement.

$$\sigma_\theta = \sqrt{14.5°\ ^2 + 2°\ ^2} = \mathbf{14.6°}$$

This is where the 14.6 value comes from in figure 8.
We took 5% of the peak maximum to be approximately isotropic background levels - almost no coicedent gamma photons should have been detected from 'background' sources due to the coicedence electronics in place. We also had to make a minor approximation for the angular region over which we measured to be **linear** in order to obtain a gradient for the line. This is shown in the denominator of the $\sigma_{\theta-Na22}$ equation.

3 Conclusions

Our results show the angular distribution of gamma decays in a Cobalt-60 source support our theoretical understanding given our calculated uncertainties. Our measurments using Sodium-22 demonstrate the maximum angular resolution obtainable from the experimental apparatus in it's current configuration. This is because the positron annihilation events are exactly correlated temporally and spatially. Ways this experiment using the same apparatus could be improved include moving the detectors further away from the source, increasing the exposure times at every angle and measuring the angle of the detectors to a higher precision. Recording at more angles (full circle) with a smaller intervals (perhaps every 5°) would produce a more continuous plot.

4 References

[1] on page 2 - accessed on March 12, 2015 - http://bit.ly/1GddaNi

[2] on page 6 - accessed on March 12, 2015 - Equation 3.11 - Section 9. Time coincedence techniques - Page 424 - Experiments in Modern Physics Academic Press 1966 - Adrian C. Mellisinos

Figure 1 on page 2 - accessed on March 12, 2015 - http://bit.ly/1CNMTHT

Figure 3 on page 3 - accessed on March 12, 2015 - Jens Maus ($http://jens-maus.de/$) - part of PhD thesis $http://nbn-resolving.de/urn:nbn:de:bsz:14-qucosa-23509$

Figure 4 on page 4 - accessed on March 12, 2015 - http://bit.ly/1wfhTOF